Title
A vascularized and perfused organ-on-a-chip platform for large-scale drug screening applications.

Journal
Lab on a chip, 17(3)

ISSN
1473-0197

Authors
Phan, Duc TT
Wang, Xiaolin
Craver, Brianna M
et al.

Publication Date
2017

DOI
10.1039/c6lc01422d

Peer reviewed

HHS Public Access

Author manuscript

Lab Chip. Author manuscript; available in PMC 2020 February 01.

Published in final edited form as:

Lab Chip. 2017 January 31; 17(3): 511–520. doi:10.1039/c6lc01422d.

A vascularized and perfused organ-on-a-chip platform for large-scale drug screening applications

Duc T.T. Phan[*,a], **Xiaolin Wang**[*,b], **Brianna M. Craver**[a], **Agua Sobrino**[a], **Da Zhao**[c], **Jerry C. Chen**[a], **Lilian Y.N. Lee**[a], **Steven C. George**[d], **Abraham P. Lee**[‡,c,e], **Christopher C.W. Hughes**[‡,a,c,f]

[a]Department of Molecular Biology & Biochemistry, University of California, Irvine, CA 92697, USA.

[b]Department of Micro/Nano Electronics, Shanghai Jiao Tong University, Shanghai, 200240, China.

[c]Department of Biomedical Engineering, University of California, Irvine, CA 92697, USA.

[d]Department of Biomedical Engineering, Washington University in St. Louis, MO 63130, USA.

[e]Department of Mechanical and Aerospace Engineering, University of California, Irvine, CA 92697, USA.

[f]The Edwards Lifesciences Center for Advanced Cardiovascular Technology, Irvine, CA 92697, USA.

Abstract

There is a growing awareness that complex 3-dimensional (3D) organs are not well represented by monolayers of a single cell type – the standard format for many drug screens. To address this deficiency, and with the goal of improving screens so that drugs with good efficacy and low toxicity can be identified, microphysiological systems (MPS) are being developed that better capture the complexity of in vivo physiology. We have previously described an organ-on-a-chip platform that incorporates perfused microvessels, such that survival of the surrounding tissue is entirely dependent on delivery of nutrients through the vessels. Here we describe an arrayed version of the platform that incorporates multiple Vascularized Micro-Organs (VMOs) on a 96-well plate. Each VMO is independently-addressable and flow through the micro-organ is driven by hydrostatic pressure. The platform is easy to use, requires no external pumps or valves, and is

cchughes@uci.edu; Fax: +1 (949) 824-8551; Tel: +1 (949) 824-8771. aplee@uci.edu; Fax: +1 (949) 824-1727; Tel: +1 (949) 824-9691.

*These authors contributed equally to this work.

‡These authors contributed equally as senior authors and correspondents to this work.

Author contributions

D.T.T.P and X.W designed and implemented the platform, performed experiments, interpreted data, and wrote the manuscript. B.M.C performed experiments, analyzed and interpreted data. A.S contributed knowledge to drug selection and the blind screening experiment. D.Z contributed to finite element simulation and platform microfabrication. J.C.C and L.Y.N.L performed experiments and analyzed data. S.C.G contributed knowledge to project development and edited the manuscript. A.P.L and C.C.W.H conceived the project, interpreted data, and wrote the manuscript. All authors read and approved the manuscript.

Conflict of interests

S.C.G, A.P.L, and C.C.W.H are founders of 4Design Biosciences, LLC.

Electronic Supplementary Information (ESI) available: [details of any supplementary information available should be included here]. See DOI: 10.1039/x0xx00000x

highly reproducible. As a proof-of-concept we have created arrayed Vascularized Micro Tumors (VMTs) and used these in a blinded screen to assay a small library of compounds, including FDA-approved anti-cancer drugs, and successfully identified both anti-angiogenic and anti-tumor drugs. This 3D platform is suitable for efficacy/toxicity screening against multiple tissues in a more physiological environment than previously possible.

Introduction

Despite continuous advances in drug screening methodology, only a small fraction of drug candidates achieve approval by the US Food & Drug Administration (FDA) for clinical use. As recently reported, over 80% of drug candidates fail during phase II and phase III clinical trials due to lack of efficacy and/or adverse events [1]. These issues are not identified during preclinical studies, largely due to the lack of effective screening methods that can mimic the complexity of human tissue and provide rapid, reliable screening readouts.

The urgent need for an innovative approach to better mimic human drug responses in preclinical studies has driven the development of “organ-on-a-chip” technologies or microphysio-logical systems (MPS). Utilizing advances in microfluidic technology and 3-dimensional (3D) cell culture techniques, these systems aim to recapitulate the complexity found *in vivo,* which includes: 3D structure; heterogeneous cellularity; cell-cell interactions; the presence of a complex extracellular matrix (ECM); perfused vasculature; and, biomechanical forces (e.g. shear forces generated by fluid flow) [2]. In recent years, efforts to develop MPS have been focused on recreating human organs such as heart, liver, lung, and brain at the level of their smallest functional unit for toxicity testing and limited drug screening [3–7]. In parallel, several “disease-on-a-chip” platforms have also been developed to model human diseases for basic science research [8, 9]. While these organ-on-a-chip platforms have demonstrated significant improvements in mimicking human organs and disease stages over traditional 2D monolayer culture systems, they are still, in many cases, at the proof-of-concept stage. Many of these platforms require complex peripheral equipment and accessories to operate and maintain, and thus may not be ideally suited for larger-scale compound screening.

Recently, we have developed methods to generate perfused, vascularized human microtissues *in vitro* [10, 11]. While we have demonstrated the use of our microfluidic system to create vascularized micro-organs (VMO) and vascularized microtumors (VMT) *in vitro* for drug screening [11], this prototype was not designed for larger-scale drug screening. Specifically, the former iteration is cumbersome with large medium reservoirs required, which necessitates a larger amount of drug. This is not practical for screening novel compounds, which during the development phase are often only synthesized in small quantities. Additionally, the 96-well plate format is compatible with standard robotic and fluorescent plate readers. To address this need we have redesigned the platform to create arrays of standardized and highly reproducible VMOs. The platform conforms to the size and arrangement of a standard 96-well plate and consists of 12 independently addressable tissue units (VMOs) with fluid flow driven by hydrostatic pressure. Each unit can be fed with a different drug or drug dose. The platform is user-friendly, does not require external

pumps or valves, is easy to load due to the incorporation of independent pressure regulator circuits [12], and requires minimal training to operate. Finally, tissues can be easily extracted from each unit for subsequent gene expression analysis. While a multitude of different tissue-specific cell types can be incorporated into the tissue, here we demonstrate the utility of the platform using colon tumor cells.

Materials & Methods

Platform design

The platform is custom-fitted into a standard 96-well plate format. The design is presented in Figure 1 and consists of two Polydimethylsiloxane (PDMS) layers assembled to a commercial 96-well plate (FLUOTRAC™ 600, Greiner Bio-One) with the bottom of specific wells removed to align with the platform (Figure 1a). The 2-mm thick middle layer consists of 12 microfluidic device units (denoted as the PDMS device layer) and the bottom layer is a thin transparent polymer membrane (HT-6240, Rogers Corp).

Since liquid evaporation at the corner and edge wells is faster than the inner wells of 96-well plates, only 12 microfluidic device units (U1-U12) are usually arrayed within the inner well area to ensure optimal culture condition. For a single unit, 6 horizontal wells (W1-W6) are utilized. The tissue unit consists of 3 tissue chambers (T1-T3) positioned within the footprint of a single well, with one gel loading inlet (L1) and outlet (L2) located at two additional wells (Figure 1b and 1c). Based on a previous design, each tissue chamber is 2 mm in length and 1 mm in width, connected to two 100-μm wide microfluidic channels through 50-μm wide capillary burst valves [11]. The tissue chambers, and the outer microfluidic channels are 100-μm deep. To facilitate a robust hydrogel loading process, an on-chip pressure regulator module with one redundant gel outlet (PR) is integrated into each unit [12]. The pressure regulator unit consists of pressure-releasing burst valves that maintain a lower burst pressure at the communication pores of the tissue chamber, and diversion channels that act as an escape route for redundant gel once the injection pressure is over the burst pressure limit. The microfluidic channels are coupled in an asymmetrical design with one medium inlet (M1) and outlet (M2) and in-line fluidic resistors, which generates interstitial flow across the tissue chambers, while minimizing the area used for each device unit on a 96-well plate (Figure 1c).

Platform fabrication

Due to the larger configuration required for the 96-well plate format, the PDMS device layer cannot be directly fabricated using soft lithography on a 3 or 4-inch SU-8 silicon mold. To address this challenge, a customized polyurethane master mold is fabricated using 2-part polyurethane liquid plastic (Smooth Cast 310, Smooth-On Inc.) and a micro-molding technique (Supplemental Figure S1a) [13]. The PDMS layer is then replicated from the customized polyurethane master mold and holes are punched for inlets and outlets (Supplemental Figure S1b). After the micro-molding process, the platform is assembled in two steps. The PDMS layer is first attached to the bottom of a 96-well plate by a chemical gluing method [14]. Briefly, the plastic bottom of the 96-well plate is immersed into a 2% (v/v) aqueous solution of 3-mercaptopropyl trimethoxysilane (Sigma-Aldrich) diluted in

98% methanol, for 1 minute. After hydrolysis and nucleophilic reaction, the alkoxysilane-terminated substrate on the plastic bottom is rinsed with distilled water and dried with nitrogen. The surface-modified well plate and the PDMS layer are then treated with oxygen plasma for 2 minutes, aligned, and bonded together. The 150-μm thin transparent membrane is then bonded to the bottom of the PDMS device layer by treating with oxygen plasma for an additional 2 minutes. To stabilize the bottom layer, the plastic protective sheet on one side of the polymer membrane is kept, while the other side is removed to allow bonding to the PDMS device layer. This protective sheet replaces the glass coverslip traditionally used for microfluidic devices. Although the glass coverslip provides better mechanical support, it hinders the extraction of cells within the tissue chambers for further molecular analysis. The fully assembled platform (Supplemental Figure S1c) is placed in 60^{o}C oven overnight, covered with a standard 96-well plate polystyrene lid, and sterilized using UV light for 30 minutes prior to use. A low-power view of 3 tissue chambers inside a single well is shown in Supplemental Figure S1d.

Cell culture

Human endothelial colony-forming cell-derived endothelial cells (ECFC-EC) are isolated from cord blood as previously described and with IRB approval [15]. After selection for the CD31+ cell population, ECFC-EC are expanded on fibronectin-coated flasks and cultured in EGM-2 (Lonza). ECFC-EC are then transduced with lentiviruses encoding various fluorescent proteins (mCherry/Addgene: C2 or Venus-GFP/Addgene: V2) and used between passages 4–6. Human normal lung fibroblasts (NHLF) are purchased from Lonza and cultured in DMEM (Corning) containing 10% FBS (Gemini Bio). NHLF are used between passages 6–8. HCT116 colorectal cancer cells, a gift from the UC Irvine Chao Family Comprehensive Cancer Center, are transduced with lentiviruses encoding various fluorescent proteins (including Azurite Blue/Addgene: Azurite). Cells are cultured in DMEM (Corning) containing 10% FBS (Gemini Bio). All cells are cultured at 37^{o}C/20% O_2/5%CO_2.

Loading of tissue chambers

VMO and VMT are established in the platform as previously described [11]. Briefly, ECFC-EC and NHLF are harvested and resuspended at a 1:1 ratio for a final density of 10^7 cells/mL in 10 mg/mL fibrinogen solution (Sigma-Aldrich). The cell-matrix mixture is quickly mixed in 3U/mL thrombin and loaded into the tissue chambers of each unit on the platform. By integrating a pressure regulator unit, the fibrin gel is confined inside the tissue chamber with a smooth gel-air interface at the capillary burst valve. After allowing gel polymerization for 15 minutes, microfluidic channels are coated with mouse natural laminin (1 mg/mL, Thermo Fisher) for 15 minutes before replacing with cell culture medium EGM-2 (Lonza). Hydrostatic pressure is established at the inlet and outlet medium reservoir wells to generate laminar flow along the microfluidic channels and the interstitial flow across tissue chambers. Hydrostatic pressure is restored to initial levels, and flow direction is switched, every 24 hours to ensure constant culture medium flow and bi-directional cell stimulation. Medium is replaced every other day after embedding.

Immunostaining

The platform is fixed for immunostaining by perfusing 4% paraformaldehyde (PFA) through the medium inlet for 30 minutes at room temperature. After fixing, PFA is replaced with 1x DPBS to wash for 1 hour at room temperature, or overnight at 4ºC. The platform is inverted and the bottom polymer membrane is carefully removed. Subsequent procedures are performed using a micropipettor. Each tissue units are washed with 1x DPBS once before permeabilizing for 15 minutes with 0.5% Triton-X100 diluted in DPBS. After permeabilization, tissue units are blocked with 10% goat or donkey serum for 1 hour at room temperature. Each tissue unit are then incubated with polyclonal rabbit anti-human Claudin-5 (Abcam) or rabbit anti-human VE-Cadherin (Enzo Life Sciences) primary antibodies (1:2000 dilution in 5% serum) for 1 hour at room temperature. After washing with 1x DPBS, tissue units are incubated with goat or donkey anti-rabbit secondary antibodies (1:2000 dilution in 5% serum) for 45 minutes before washing with DPBS and counter-staining with DAPI. Finally, anti-fade solution is added on top of each tissue unit before mounting with a glass coverslip.

Finite Element Simulation

Finite element simulations for interstitial flow through ECM embedded in the tissue chamber is performed using COMSOL Multiphysics 5.0 (Comsol Inc., Burlington, MA, USA). The Brinkman's equation is employed for momentum transportation through a porous fibrin gel with low permeability (1.5×10^{-13} m^2) confined in the tissue chamber, and is driven by the hydrostatic pressure drop over a period of 24 hours, as previously described [16].

Drug exposure studies

Each device unit containing VMO or VMT is exposed to a standard primary screening concentration of 1 μM. Compounds are obtained from the National Cancer Institute (NCI) Approved Oncology Compound Plate or purchased from Selleck Chemicals. All compounds are dissolved in dimethyl sulfoxide (DMSO) and diluted in the culture medium with less than 0.01% DMSO. For a standard primary screening assay, after culturing for 7 days to allow full development of each tissue unit, culture medium is replaced by medium containing the drugs at the desired concentration, and delivered through the microfluidic channels using the hydrostatic pressure gradient. Hydrostatic pressure is restarted and flow direction is switched every 24 hours. Tissues are exposed to compounds for 72 hours before quantifying the effect on total vessel length and tumor growth.

Cell viability in response to drugs in 2D monolayer cultures is quantified using an XTT assay. Briefly, 10,000 cells (ECFC-EC or HCT116) are seeded in triplicate in a 96-well plate and allowed to grow for 24 hours prior to treatment with drugs at 1 μM. XTT assays are performed after 72 hours of drug exposure and cell viability is normalized to control wells without drug treatment according to the manufacturer's protocol (Sigma-Aldrich).

Time-lapse imaging and time course analysis

Time-lapse image sequences and time course images are taken using a Nikon Ti-E Eclipse epifluorescent microscope with a 4x Plan Apochromat Lambda objective. For close-up

imaging of the tissue chambers, a 1.5x intermediate magnification setting is used. For vessel quantitative analysis, total vessel length and vessel percentage area are quantified using AngioTool (National Cancer Institute). For tumor growth quantitative analysis, fluorescent intensity is processed and analyzed using ImageJ (National Institute of Health). Briefly, images are thresholded to select for the fluorescent tumor region, and the mean fluorescence intensity is measured within the threshold region. Tumor total fluorescent intensity is defined as the product of the fluorescent area and the mean fluorescent intensity within that region. Final values of vessel and tumor growth quantitative analysis are normalized to initial values at time zero of drug exposure. Three replicates (tissue units) are examined per experiment. Confocal imaging of fluorescent immunostaining is performed on a Leica TCS SP8 confocal microscope using a 20x multi-immersion objective with 2x digital zoom setting. Where adjustments are made to images, these are performed on the entire image, and all images in that experimental group are adjusted to the same settings.

RNA isolation and qRT-PCR analysis

For RNA isolation, the plastic cover underneath the platform is removed and the PDMS region containing the 3 tissue chambers is extracted using a sterile scalpel. Each PDMS piece is transferred into a 1.5 mL tube and resuspended in Trizol for cell lysis. Supernatant is then transferred into a new 1.5 mL tube to extract RNA. Isolated RNA is treated with Turbo DNase (Invitrogen) for 20 minutes. Total purified RNA is synthesized into cDNA using iScript cDNA Synthesis Kit (BioRad) and used for quantitative real-time polymerized chain reaction (qRT-PCR). Average cycle threshold (Ct) values are normalized to 18S expression levels and all samples are measured in triplicate. Primers are designed using PrimerQuest Tool and synthesized by Integrated DNA Technologies. Primer sequences are listed in the Supplemental Table 1.

Statistical Analysis

Data are shown as mean ± standard deviation unless stated. Estimated means, and standard deviation are calculated using Microsoft Excel. Comparison between experimental groups of equal variance is analyzed using Student’s t-test or one-way ANOVA followed by Dunnett’s test for multiple comparisons using GraphPad Prism 7.0. Number of replicates is indicated in the legends. The level of significance is set at $p < 0.05$.

Results

Finite element simulation of interstitial flow required to induce vasculogenesis

VMOs are generated in this platform through the process of vasculogenesis. In a previous study, we have demonstrated the importance of interstitial flow and the optimal conditions to induce vasculogenesis [16]. We performed time-dependent flow simulations to optimize the hydrostatic pressure, as this device is limited to the smaller volume that a single well can hold (maximum volume: 382 uL) compared to a larger volume in the plastic/glass medium reservoir previously utilized (Figure 2). To maximize the interstitial flow duration, the inlet medium volume was initially set to V_{inlet} = 382 uL (P_{inlet} =10.9 mmH_2O or 106.82 Pa) correlating with the maximum well volume, and the outlet medium volume was set to V_{outlet} = 50 μL (P_{outlet} = 1.38 mmH_2O or 13.52 Pa) correlating with the minimum volume after

accounting for liquid evaporation. Figure 2a shows hydrostatic pressure (color scale) and flow velocity profile (streamline) in a whole tissue unit at steady state. Interstitial flow across the tissue chamber was then examined to determine if it is sufficient to induce vasculogenesis, based on the limits we previously established [16]. Because of the coupled microfluidic channel design, the hydrostatic pressure difference at the inlet and outlet reduces over time, leading to reduction in interstitial flow. This gives rise to concern of insufficient induction of vasculogenesis inside the tissue chambers. To address this issue, flow simulation was performed for 24 hours with the initial hydrostatic pressure setting (Supplemental Video 1). The hydrostatic pressure and interstitial flow velocity in both vertical (Figure 2b) and horizontal (Supplemental Figure S2) directions are within the optimal range (0.1 – 11 μm/s) previously reported [16] to continuously induce vasculogenesis. As shown in Figure 2B, each line represents the hydrostatic pressure and interstitial flow velocity vertically across a tissue chamber from time T=0 hour to T=24 hours. Over the course of 24 hours, the hydrostatic pressure difference is maintained between 8 to 19 Pa (0.82 to 1.94 mmH_2O), and the interstitial flow velocity is maintained between 1.22 to 22.36 μm/s. In Supplemental Figure S2, flow simulation in the horizontal direction across a tissue chamber indicates that the hydrostatic pressure difference is uniform, ranging between 57.8 and 59.2 Pa (5.89 to 6.03 mmH_2O), and the interstitial flow velocity is maintained between 0.37 and 2.67 μm/s. A summary of the flow simulation is shown in Table 1. We conclude from these studies that if the hydrostatic pressure difference at the medium inlet and outlet is reset every 24 hours, then sufficient interstitial flow is maintained across the tissue chambers to induce vasculogenesis.

Generation of vascularized tissues is highly reproducible

Three important factors were considered when designing the platform: user-friendliness, reproducibility, and robustness. Although monolayer and spheroid screening systems do not accurately represent tissue complexity, they are still widely adopted due to their simplicity and user-friendliness. Microfluidic systems, while providing a dynamic flow environment, often require additional equipment to support the microfluidic device, as well as extensive user training. To address these issues, the flow system utilized in our platform is solely driven by hydrostatic pressure, thus eliminating the need for external pumps and tubing. In addition, to improve user-friendliness and reproducibility, an on-chip pressure regulator that facilitates reproducible hydrogel loading was integrated into each unit on the platform [12]. This integration has minimized the required training time to successfully embed the cell-matrix mixture into each unit down to a single day, thereby alleviating a major bottleneck in our earlier studies. The process is highly reproducible with, on average, 11 out of 12 units successfully loaded on each platform.

Successfully loaded device units developed robust and uniform vascular networks within 7 days. Figure 3a shows vascular networks formed inside the 3 tissue chambers on Day 7. To confirm vascular perfusion, 70-kDa FITC dextran (25 μg/mL) was introduced to the medium inlet and tissue units were monitored for 30 minutes. As shown in the same figure, 70-kDa dextran was perfused throughout the vasculature in the three tissue chambers. Perfusion is highly consistent in 12 tissue units within a single platform, as shown in Supplemental Figure S3. While anastomotic connections between the vascular networks and the

microfluidic channels formed naturally in all 12 tissue units, the seal is not always as tight as we see when lining EC inside the microfluidic channels [10]. Immunostaining of tight junctions (Claudin-5) and adherens junctions (VE-Cadherin) on Day 7 post-embedding in Figure 3b and 3c demonstrated a mature, high integrity vasculature.

The vessel area percentage and total vessel length in each tissue chamber were quantified to assess vascular formation on a successfully loaded platform (Figure 4). Quantification demonstrated that the percent vessel coverage and total vessel length between the tissue chambers (n= 36 tissue chambers) in a single platform (n= 12 units) are highly consistent, with a coefficient of variation (CV) equal to 10.2% and 9.8%, respectively (Figure 4a). To further assess the reproducibility between different platforms, the average percent vessel coverage and total vessel length of each unit on two independent platforms were quantified (Figure 4b). These are also consistent, with CV equal to 12.4% and 11.9% respectively. We compared these CVs to a standard 2D assay. We plated 10,000 fluorescent-tagged EC into each well of two 96-well plates (n=36 wells, 2 plates) and allowed the cells to adhere for 2 hours. Fluorescent intensity was then measured in each well using a fluorescent plate reader. The calculated CV for these monolayer cultures in 2 independent well plates was 12.8% (Supplemental Figure S4). Thus the calculated CVs of 2D monolayer culture versus complex 3D cultures in our platform are compatible, showing that our system is highly robust and reproducible.

Analysis of gene expression in the platform

An important advance over previous iterations of the platform, which were also limited to single units versus the twelve we have here, is our ability to extract RNA for gene expression analysis. To demonstrate the potential of the platform for gene expression analysis, units were challenged with TNF-α (20 ng/mL, n=12) for 24 hours, or were left untreated (n=12), and total RNA was extracted for analysis of VCAM-1, E-Selectin, and ICAM-1 by qRT-PCR. TNF-α is a known strong inducer of all three genes in EC [17]. Figure 5 shows average gene expression levels of TNF-α treated cells compared to control, from 3 independent experiments. Consistent with previous reports [16], TNF-α increased expression of VCAM-1 (average 2.4 fold), E-Selectin (average 3.3 fold), and ICAM-1 (average 6.8 fold). These results demonstrate the potential use of our platform for studying gene expression levels in a 3D, vascularized and perfused tissue *in vitro*.

Drug screening validation

We have previously reported a vascularized tumor model using an early iteration of our microfluidic platform and demonstrated its application for anti-cancer drug screening [11]. To demonstrate the potential use of our platform for anti-cancer drug screening at a larger scale, the colorectal cancer cell line HCT116 was embedded with EC and stromal cells to create a VMT in each device unit. The VMTs were allowed to develop for 7 days prior to drug exposure. To confirm vascular perfusion in each VMT, 70-kDa Rhodamine B dextran (25 ug/mL) was introduced to the medium inlet and tissue units were monitored for 30 minutes (Figure 6a). All 12 VMTs within a single platform had perfused vascular networks (Supplemental Figure S5).

A blinded, primary drug screening at 1 μM concentration was performed using a panel of FDA-approved anti-cancer compounds aliquoted and coded by an investigator not involved in this study: Bortezomib, Vincristine, CP-673451, Linifanib, Tamoxifen, Axitinib, Sorafenib, Mitomycin C, Vorinostat, and Gemcitabine. For negative control compounds, Isoprenaline and Propranolol were chosen. A summary of these compounds and their targets is shown in Supplemental Table 2. VMTs were allowed to develop for 7 days before exposure to drugs. Images of vasculature and tumors were captured before drug treatment to compare drug effects after 72 hours. As shown in Figure 6b, tested compounds showed a wide range of efficacy. Representative images before and after 72 hours of drug treatment are shown in Figure 6c and Supplemental Figure S6. Isoprenaline and Propranolol, two negative control compounds, showed no effect on either tumor growth or the vasculature. Bortezomib and Linifanib effectively targeted both tumor growth and the vasculature. Other compounds have preferential effects on either tumor growth or the vasculature. Tamoxifen, Mitomycin C, Gemcitabine, and Vorinostat were more effective in targeting tumor growth, while Vincristine and Axitinib showed preferential effects on targeting the vasculature. Over longer treatment times targeting the vasculature also reduces tumor growth due to reduced nutrient supply [11].

We performed power calculations based on these data, with an alpha (significance level) of 0.05 and a power of 0.8, for both anti-vessel and anti-tumor responses. For drugs such as bortezomib, vincristine, mitomycin C, gemcitabine, vorinostat and tamoxifen the required number of replicates for seeing anti-tumor effects was 4–7, well within the range of the platform. When assaying for anti-vascular effects we found that the required number of replicates for Bortezomib, Vincristine, Linifanib, Axitinib and Sorafenib was 2–4, again well within the range of the platform.

Tumor cells and EC behave quite differently in 2D cultures than they do in 3D [11] and so we compared the efficacy of the above panel of drugs against the same tumor cells and EC used above, but in 2D monolayer cultures. Perhaps not surprisingly we saw dramatic differences (Supplemental Figure S7), including the ineffectiveness of drugs such as Mitomycin C, Gemcitabine, and Vorinostat on HCT116 cells in 2D compared to their strong anti-proliferative effects in the VMT. Similarly, several drugs were detrimental to EC viability in 2D but had little to no effect on vascular stability in 3D cultures.

In conclusion, highly reproducible VMTs can be grown in this platform and used for drug screening with robust readouts for drug efficacy on tumor growth and the associated vasculature.

Discussion

The development of this platform represents a significant advance in the development of drug discovery tools. Building on our previous work that generated *in vitro* perfused, vascularized microtissues, we have standardized the platform design to fit into a 96-well plate format, making it more suitable for larger-scale drug screening applications. One of the major advantages of this platform compared to other microphysiological systems is its simple, user-friendly design that requires no external pumps or tubing, and minimal user

training to load and operate. The platform is compact and can be easily transferred between laboratories, requiring no additional equipment beyond a standard incubator. Highly reproducible, living vascular networks form inside the tissue chambers allowing for a more physiologic representation of human tissues than has been previously possible in other drug-screening platforms. A small fluid volume requirement for each tissue unit allows for large-scale primary drug screenings at low cost. In particular, for novel compound development, where compound synthesis is expensive, only a small quantity of the compound is required. In addition, RNA extraction from the tissue chambers allows for gene expression analysis and probing of mechanism.

A power analysis based on the data presented here suggests that for compounds with efficacy similar to those tested, a number of replicates between 3 to 7 may well be sufficient to reliably identify hits. For smaller effects the number of replicates may be unreasonably high. This, combined with the higher complexity of the platform compared to standard 96- or 384-well plate assays, leads us to conclude that the VMT platform will be better suited to preclinical testing of a smaller subset of compounds (<100) rather than screens of large libraries containing tens of thousands of compounds.

While the VMT platform has many advantages, there are still some limitations in our approach. First, due to the limited volume of the wells in a 96-well plate, the optimal hydrostatic pressure difference cannot be maintained for more than 24 hours. As a result, it is necessary to add additional medium each day to maintain the hydrostatic pressure head and a constant fluid flow rate. However, this could be addressed in future work by customizing a taller 96-well plate that can hold more volume per single well, or a plug-in adapter to increase the well depth for the standard 96-well plate.

Second, because of a smaller hydrostatic pressure difference between the inlet and outlet, the flow velocity generated in this platform is approximately twice lower than the physiological blood flow velocity through capillaries [18], resulting in a lower shear stress exerted on the vascular wall. Our estimation for shear stress exerted on the vascular wall in this platform is 2 to 3 times lower than what vascular capillaries experience *in vivo* [19]. Thus the platform has some limitations when studying the effects of shear stress on vascular gene expression and morphology. However, it is worth noting that shear stress is the product of flow rate and fluid dynamic viscosity. Blood is a non-Newtonian fluid with high fluid dynamic viscosity, thus the shear stress exerted on the vascular wall *in vivo* is higher than cell culture medium, a Newtonian fluid that is comprised mainly of water. A higher shear stress could be achieved with the current flow rate if the cell culture medium is modified to increase its dynamic viscosity, something we are currently examining.

It should be noted that the vasculature in the VMTs is leakier compared to the vasculature in VMOs discussed earlier, and the degree of leakiness varies widely between each VMT on a single platform. This phenomenon is perhaps not surprising, as tumor-associated vasculature is known to be leakier than normal vasculature [20]. Thus the VMTs in this platform may be a useful model of the tumor microenvironment *in vivo*.

Although the screening readout is robust, manual operations under the microscope are still required for drug efficacy analysis. Thus, before the platform becomes truly useful for screening with a larger set of compounds the quantification and data analysis processes needs to be automated. This can be done through a customized fluorescent plate reader, or an automated microscope camera system to capture images at different time points. In addition, a machine-learning algorithm can be utilized to interpret data and predict potential "hit" candidates for secondary screening. We are currently exploring these approaches.

Conclusions

In this paper, we have presented a novel organ-on-chip platform comprising human vascularized microtissues suitable for drug screening applications. The platform is custom-fitted to a standard 96-well plate format with a simple, easy-to-operate design. Vascularized microtissues grown in this platform are highly reproducible and the vasculature is fully functional. In addition, RNA can be extracted from the tissues for gene expression analysis. Finally, we show that the VMT platform can successfully identify anti-cancer and anti-vascular drugs. This platform is an advance in the field of organ-on-chip research and it will be a useful tool for drug discovery.

Supplementary Material

Refer to Web version on PubMed Central for supplementary material.

Acknowledgements

The authors would like to thank Chinh Tran for help with microfabrication, and Michaela Shuler Hatch and Kimberly Lim for help with cell isolation. This work was supported by grants from the National Institutes of Health: R01 CA180122 (PQD5), and UH3 TR00048. C.C.W.H receives support from the Chao Family Comprehensive Cancer Center (CFCCC) through an NCI Center Grant award P30A062203. X.W receives support from National Natural Science Foundation of China (No. 31600781).

References

1. Arrowsmith J and Miller P, Nat Rev Drug Discov, 2013, 12, 569. [PubMed: 23903212]
2. Fabre K, Livingston C and Tagle D, Exp Biol Med (Maywood), 2014, 239, 1073–1077. [PubMed: 24962171]
3. Brown J, Pensabene V, Markov D, Allwardt V, Neely M, Shi M, Britt C, Hoilett O, Yang Q, Brewer B, Samson P, McCawley L, May J, Webb D, Li D, Bowman A, Reiserer R and Wikswo J, Biomicrofluidics, 2015, 9.
4. Esch M, Ueno H, Applegate D and Shuler M, Lab Chip, 2016, 16, 2719–2729. [PubMed: 27332143]
5. Huh D, Matthews B, Mammoto A, Montoya-Zavala M, Hsin H and Ingber D, Science 2010, 328, 1662–1668. [PubMed: 20576885]
6. Mathur A, Loskill P, Shao K, Huebsch N, Hong S, Marcus S, Marks N, Mandegar M, Conklin B, Lee L and Healy K, Sci Rep, 2015.
7. Shi P, Scott M, Ghosh B, Wan D, Wissner-Gross Z, Mazitschek R, Haggarty S, and Yanik M, Nat Commun, 2011, 2.
8. Jeon J, Bersini S, Gilardi M, Dubini G, Charest J, Moretti M and Kamm R, Proc Natl Acad Sci U S A, 2015, 112, 214–219. [PubMed: 25524628]
9. Kim H, Li H, Collins J and Ingber D, Proc Natl Acad Sci U S A, 2016, 113, E7–15. [PubMed: 26668389]

10. Wang X, Phan D, Sobrino A, George S, Hughes C and Lee A, Lab Chip, 2016, 16, 282–290. [PubMed: 26616908]
11. Sobrino A, Phan D, Datta R, Wang X, Hachey S, Romero-López M, Gratton E, Lee A, George S and Hughes C, Sci Rep, 2016.
12. Wang X, Phan D, Zhao D, George S, Hughes C and Lee A, Lab Chip, 2016, 16, 868–876. [PubMed: 26879519]
13. Desai S, Freeman D and Voldman J, Lab Chip, 2009, 9, 1631. [PubMed: 19458873]
14. Wu W, Wu J, Kim J and Lee N, Lab Chip, 2015, 15, 2819–2825. [PubMed: 26014886]
15. Melero-Martin J, Khan Z, Picard A, Wu X, Paruchuri S and Bischoff J, Blood, 2007, 109, 4761–4768. [PubMed: 17327403]
16. Hsu Y, Moya M, Abiri P, Hughes C, George S and Lee A, Lab Chip, 2013, 13, 81–89. [PubMed: 23090158]
17. Mackay F, Loetscher H, Stueber D, Gehr G and Lesslauer W, J Exp Med, 1993, 177, 1277–1286. [PubMed: 8386742]
18. Ivanov K, Kalinina M and Levkovich Y, Microvasc Res, 1981, 22, 143–155. [PubMed: 7321902]
19. Papaioannou T and Stefanadis C, Hellenic J Cardiol, 2005, 46, 9–15. [PubMed: 15807389]
20. McDonald D and Baluk P, Cancer Res, 2002, 62, 5381–5385. [PubMed: 12235011]

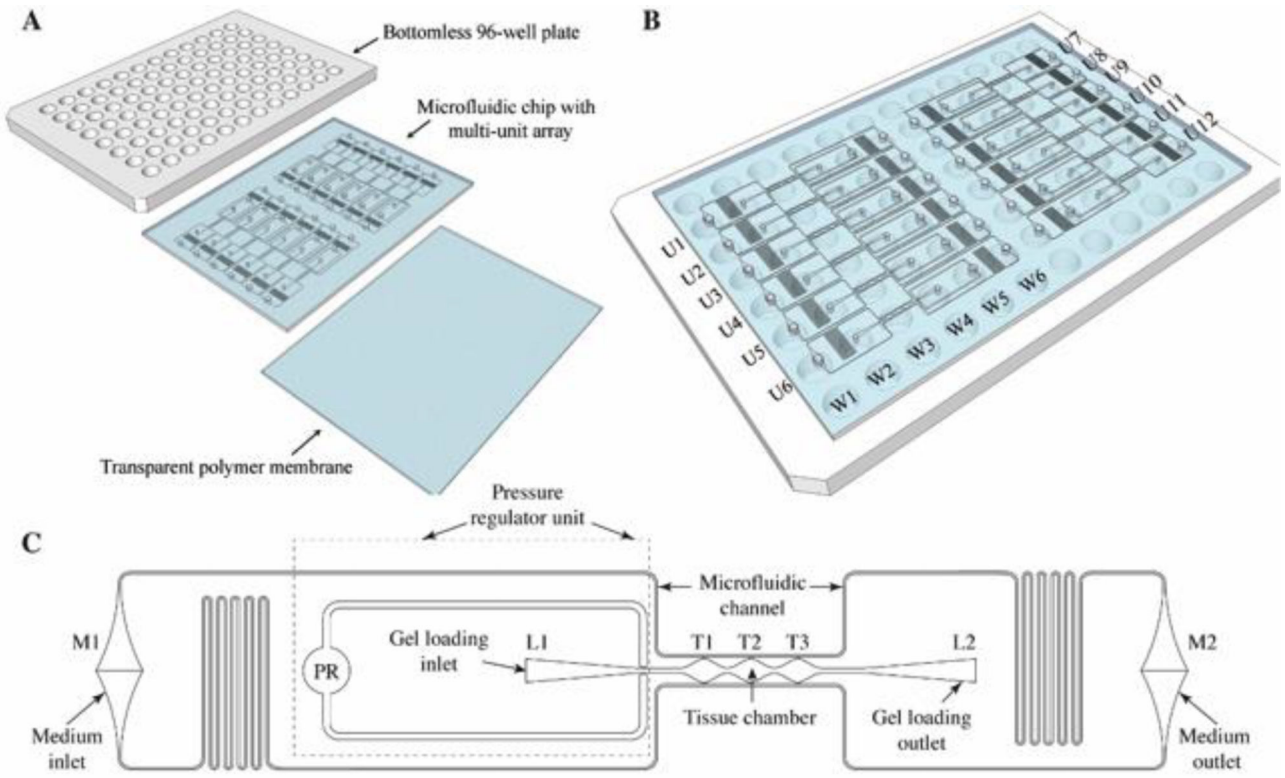

Figure 1:

Microfluidic platform design. (A) Schematic of the platform assembly. The PDMS layer containing the microfluidics, and a transparent polymer membrane are bonded to a bottomless 96-well plate. (B) Schematic of a fully assembled platform (viewed from below), with 6 tissue units arranged on half of the well plate (U1-U6), and another 6 tissue units arranged on the opposite side. Each tissue unit occupies 6 horizontal wells (W1-W6). In practice, tissue is loaded through U1/W2 or U1/W4, and medium flows from U1/W1 to U1/W6. The pressure regulator outflow occupies U1/W5. (C) Schematic of one tissue unit, which consists of 3 tissue chambers (T1-T3) connected to 2 adjacent microfluidic channels, 2 gel loading ports (L1-L2), 2 medium ports (M1-M2), and one pressure regulator unit (PR).

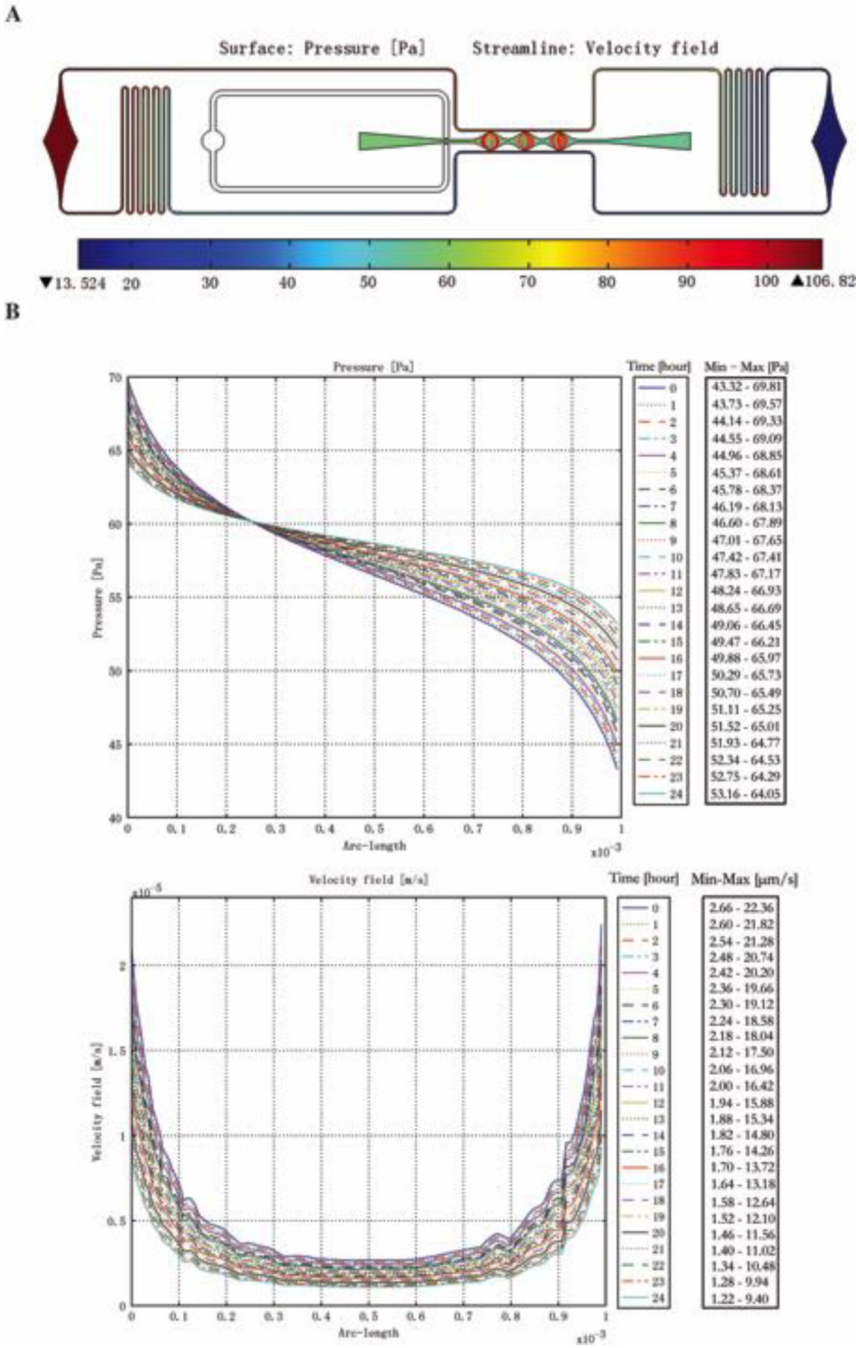

Figure 2:

Finite element simulation of the interstitial flow required to induce vasculogenesis. (A) Simulated hydrostatic pressure (Color scale. Unit : Pa) and flow velocity (Streamline) of a whole tissue unit at steady state. (B) Simulated hydrostatic pressure (Unit : Pa) and flow velocity (Unit : m/s) in vertical direction across a tissue chamber from time t = 0 hour to t = 24 hours.

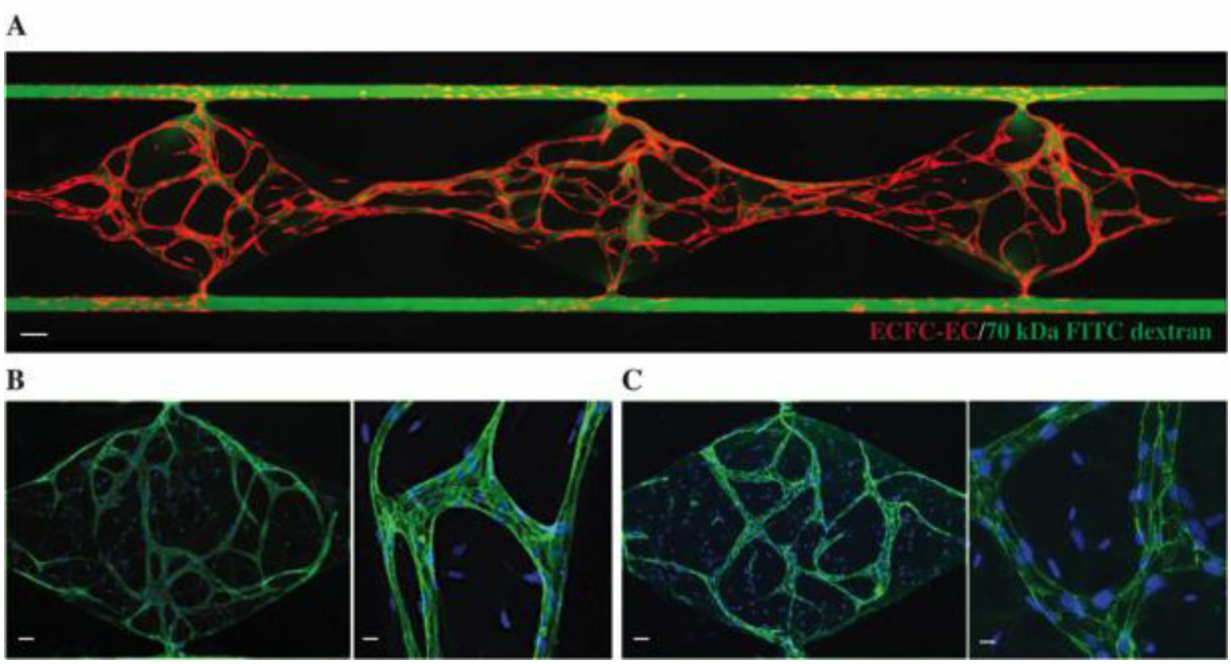

Figure 3:

Vascular network formation inside one tissue unit. (A) ECFC-EC (mCherry) formed vascular networks inside the 3 tissue chambers on Day 7. 70 kDa FITC-dextran was introduced to the medium inlet and allowed to perfuse through the vasculature for 30 minutes. Scale bar = 100 μm. (B) Immunostaining of Claudin-5 (Alexa Fluor 488) and DAPI for nuclei under 4x and 20x microscope objectives. Scale bar = 50 μm. (C) Immunostaining of VE-Cadherin (Alexa Fluor 488) and DAPI for nuclei under 4x and 20x microscope objectives. Scale bar = 50 μm.

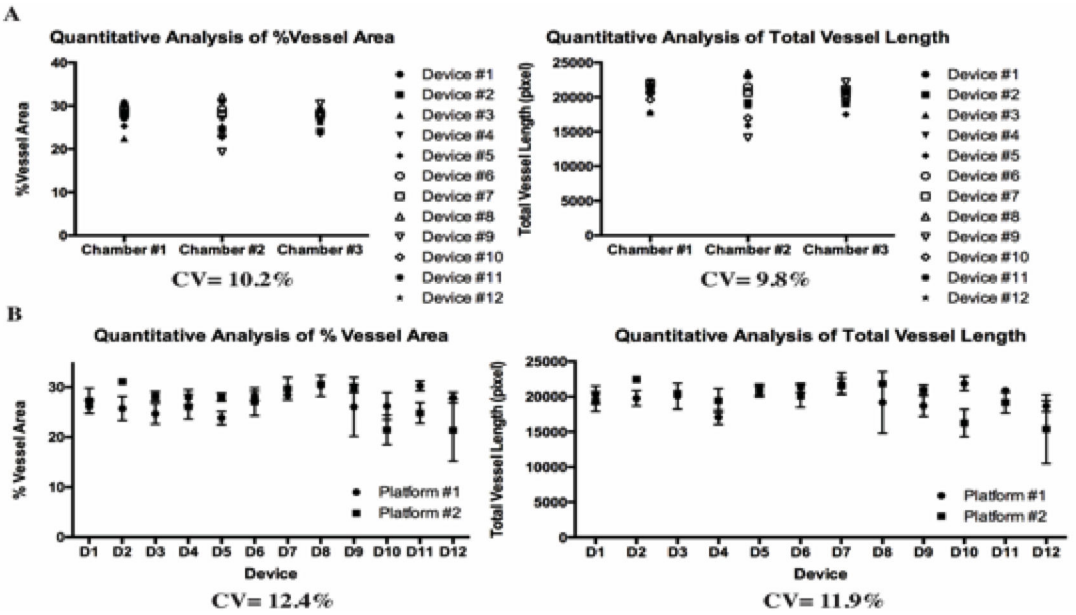

Figure 4:

Quantitative analysis of vascular networks formed inside the platform. (A) Quantitative analysis of percentage vessel area and total vessel length between the tissue chambers (n= 36 tissue chambers) in a single platform (n=12 tissue units). (B) Quantitative analysis of the average percentage vessel area and total vessel length of each tissue unit on 2 independent platforms.

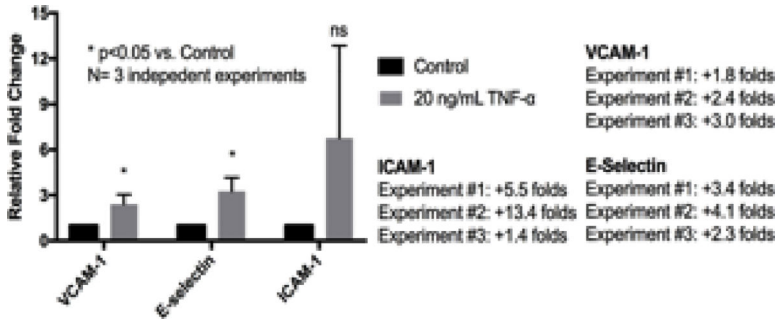

Figure 5: Gene expression analysis of VCAM-1, E-Selectin, and ICAM-1 in the platform.
Tissue units were treated with TNF- α (20 ng/mL) for 24 hours and RNA was extracted for qRT-PCR analysis. Data represent mean values of 3 independent experiments ± SEM.

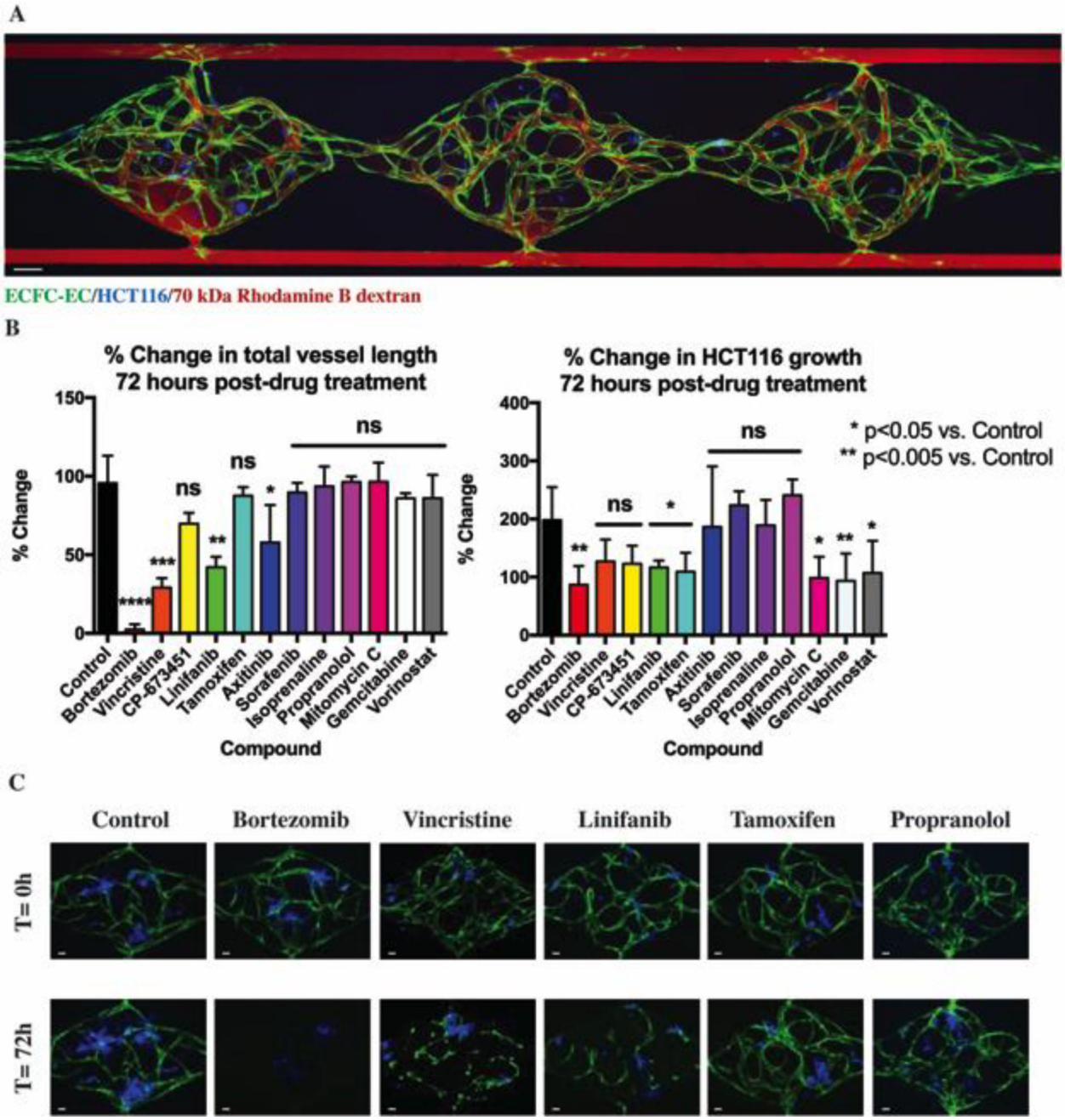

Figure 6: VMT in the platform and drug screening validation.

(A) ECFC-EC (Venus) formed vascular networks inside the 3 tissue chambers around the HCT116 colorectal cancer cells (Azurite) on Day 7. 70 kDa Rhodamine B-dextran was introduced to the medium inlet and allowed to perfuse through the vasculature for 30 minutes. Scale bar = 100 μm. (B) Primary drug screening was performed on VMTs after 7 days of culture. On Day 7, 1 μM concentration of 12 compounds was added to the medium inlet and allowed to perfuse through the vasculature. Drug efficacy on tumor growth and the associated vasculature was quantified after 72 hours. Data are shown as mean ± standard

deviation of 4 replicates per compound. (C) Representative images before (t=0h) and after (t=72h) of drug treatment. Scale bar = 50 μm

Table 1:
Summary of flow simulation at time t = 0 hour and t = 24 hours.

Units are converted to mmH_2O (pressure) and μm/s (flow velocity) for comparison to reported results [16].

Flow characteristics \ Time	T = 0h	T = 24h
Hydrostatic pressure drop between media inlet and outlet	9.52 mmH_2O (93.296 Pa)	3.95 mmH_2O (38.71 Pa)
Average flow velocity inside microfluidic channel	650 μm/s	270 μm/s
Interstitial flow range inside tissue chamber	Vertically: 2.66 – 22.36 μm/s Horizontally: 0.897 – 2.67 μm/s	Vertically: 1.22 – 9.40 μm/s Horizontally: 0.369 – 1.23 μm/s